Talanta 85 (2011) 117–122

Contents lists available at ScienceDirect

Talanta

journal homepage: www.elsevier.com/locate/talanta

A highly sensitive electrochemical immunosensor based on coral-shaped AuNPs with CHITs inorganic–organic hybrid film

Jian Tang, Rong Hu, Zai-Sheng Wu, Guo-Li Shen*, Ru-Qin Yu

State Key Laboratory for Chemo/Biosensing and Chemometrics, College of Chemistry and Chemical Engineering, Hunan University, Changsha, PR China

ARTICLE INFO

Article history:
Received 7 December 2010
Received in revised form 11 March 2011
Accepted 17 March 2011
Available online 15 April 2011

Keywords:
Coral-shaped AuNPs
Chitosan
Immunosensor
Gold nanoparticles

ABSTRACT

A highly sensitive electrochemical immunosensor based on combination of chitosan (CHIT) and coral-shaped AuNPs (C-AuNPs) to form an immobilization matrix has been developed using human IgG as a model analyte. The inorganic–organic hybrid film with abundant adsorbing sites and large surface area can reserve the biocompatibility of the biomaterials which greatly increase loading amounts of assembling, thus, significantly improves the performance of biosensing. The morphology is studied by scanning electron microscopy (SEM). Under the optimized experimental conditions, the immunosensor exhibits excellent performance (e.g., a detection limit of 5 pmol L^{-1}, a linear dynamic range of 3 orders of magnitude, high specificity). This possibly makes it an attractive platform for the direct immunoassay of human IgG or other biomolecules.

1. Introduction

Nanostructure materials are very attractive due to their unique optical, electrical, catalytic and magnetic properties potentially applicable in nanoelectronic devices, nanosensors and catalysts. Recently, gold nanoparticles (AuNPs) have become one class of the most widely studied nanostructure materials due to their advantage of easy synthesis, low cost, good biocompatibility and ability to be readily surface, modified by a variety of chemical methods [1–3]. For example, the AuNPs used in signal amplification for preparation of electrochemical biosensor has gained enormous interest [4–7], most of them are based on AuNPs assembled on the working electrode to increase the surface area, thought the improvement of the electrode performance might be rather limited as only a small quantity of AuNPs fixed on the electrode surface [4].

The seed-mediated growth methods have drawn much attention in recent years due to their fine control of nanomaterial fabrication, especially metal nanomaterials. Specifically, small size of nanoparticles might serve as the nucleation centers (seeds) to grow nanomaterials to a desired size and shape after the addition of a growth solution containing a controlled amount of metal salt, weak reducing agent (e.g., ascorbic acid), and surfactant-directing agent (e.g., cetyltrimethylammonium bromide, CTAB). Fine control of augmented particles with a desired shape can be achieved by controlling the concentration of the seed and the mole ratio of the ingredients of the growth solution [8,9]. The seed-mediated growth methods are commonly used in the preparation of nanomaterials in solution, however, there are very few reports [10,11] on the use of fabrication of biosensors. In this paper, coral-shaped AuNPs (C-AuNPs) were synthesized by using a seed-mediated growth method, the morphology of which was studied by scanning electron microscopy (SEM). The C-AuNPs provide much more assembling sites than the two-dimensional ordered AuNPs, significantly improving the response performance of the biosensors.

Chitosan (CHIT), a deacetylated product of chitin, is a high molecular weight polysaccharide composed mainly of β-(1,4)-linked 2-deoxy-2-amino-D-glucopyranose units and partially of β-(1,4)-linked 2-deoxy-2-acetamido-D-glucopyranose [12–14]. It has attracted great scientific interest since it is found to be a very useful functional material. CHIT exhibits significant properties, including biocompatibility, film-forming ability, adsorption properties and easy to chemical modification due to its abundant reactive amino and hydroxyl functional groups [15,16]. Because of its unique properties, it has been widely used as an immobilization matrix for biosensors, and can also be combined with AuNPs. The inorganic–organic hybrid film could reserve the biocompatibility of the material and the desirable properties of nanomaterials, which is valuable for biosensing.

Our research aimed at the seed-mediated method for fabricating AuNPs on the CHIT modified gold electrode and integrating the advantages of organic–inorganic hybrid film to obtain better sensor performance. Herein we designed an immunosensor based on the C-AuNPs combined with CHIT to form an immobilization matrix for a sandwich immunoreaction, which used human IgG as a model analyte. Scheme 1 shows the principle of immunosensor.

* Corresponding author. Tel.: +86 731 88821355; fax: +86 731 88821355.
E-mail address: glshen@hnu.cn (G.-L. Shen).

0039-9140/$ – see front matter © 2011 Elsevier B.V. All rights reserved.
doi:10.1016/j.talanta.2011.03.038

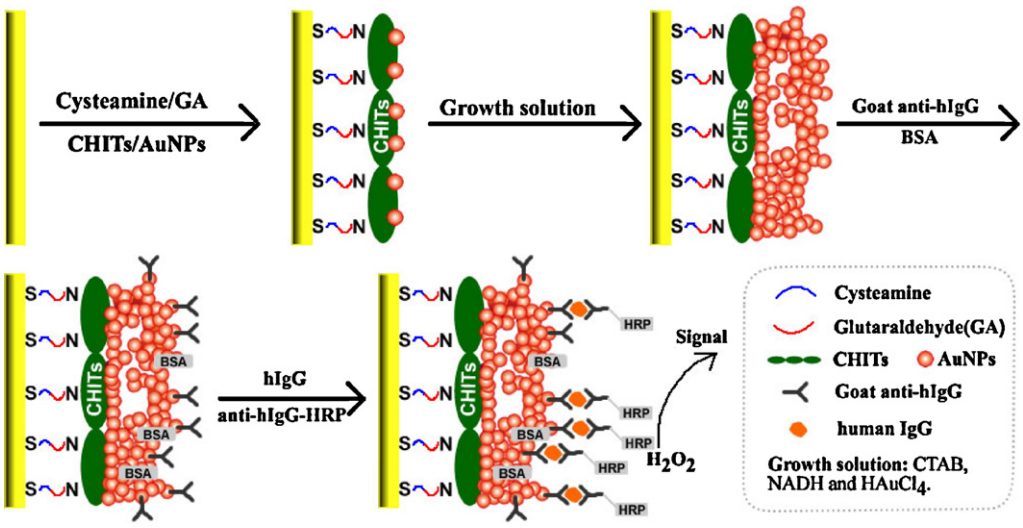

Scheme 1. Schematic illustration of the electrochemical immunosensor based on C-AuNPs (coral-shaped AuNPs)-CHITs hybrid film and enzyme amplification using the H_2O_2 system in a sandwich type.

2. Experimental

2.1. Materials and apparatus

Chitosan (CHIT) (85% deacetylated) was received from Sigma Co., Ltd. Cysteamine (Cys, 2-aminoethanethiol hydrochloride), nicotinamide adenine dinucleotide (NADH) and hexadecyltrimethylammonium bromide (CTAB) were purchased from Acros Organics (New Jersey, USA). Glutaraldehyde solution (GA) (25%) was obtained from Changsha Chemical Reagents Co. (Changsha, China). Bovine serum albumin (BSA), human IgG (hIgG), goat anti-human IgG antibody (goat anti-hIgG) and horseradish peroxidase (HRP) labelled goat anti-hIgG (goat anti-hIgG-HRP) were all purchased from DingGuo Biotechnology Co., Ltd. (Beijing, China). Phosphate buffer solution (PBS, 10 mmol L^{-1}, 0.1 mol L^{-1} KCl, pH 7.4) was used as working solution. All other reagents were of analytical reagent grade and used as received without further purification. Doubly distilled water (resistance >18 MΩ cm^{-1}) was used throughout all experiments.

All electrochemical measurements were performed using a CHI 760B electrochemical workstation (Chenhua Instruments Co., Ltd., Shanghai, China). A three-electrode system was employed consisting of a gold working electrode (2 mm diameter), a saturated calomel reference electrode (SCE) and a platinum wire auxiliary electrode. All potentials throughout experiments were reported versus the SCE.

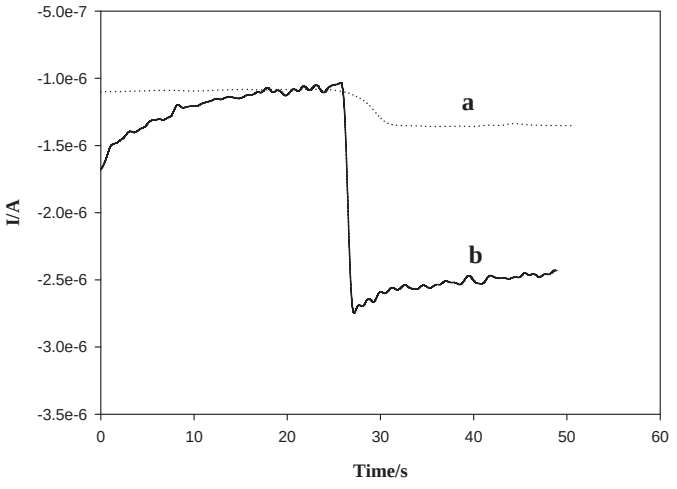

Fig. 1. Amperometric responses of the H_2O_2: in the absence (a) and presence (b) of hIgG (1 μg/ml).

2.2. Preparation of gold seeds

All glassware used was cleaned in a bath of freshly prepared aqua regia (HNO_3:HCl = 1:3, by volume) and rinsed with doubly distilled water thoroughly. AuNPs with an average diameter of 12 nm were prepared according to the literature [17]. Briefly, 1 ml of 1 (wt%) $HAuCl_4$ solution was added to 100 ml of doubly distilled water and heated under reflux keeping boiling. Then 3 ml of 1 (wt%) sodium citrate solution was added rapidly. When the solution turned to red, which indicated that AuNPs were formed, it was kept boiling for another 30 min and then cooled to room temperature with constant stirring. The AuNPs were characterized by an absorption maximum at 520 nm for AuNPs of 12 nm diameter.

2.3. Fabrication of sensing interface and seed-mediated growth process

The gold electrode was polished with 0.05-μm alumina powder, rinsed successively in an ultrasonic bath with distilled water, absolute alcohol and distilled water for 5 min each. Then the gold electrode was soaked in piranha solution (H_2SO_4:H_2O_2 = 7:3, by volume) for 15 min. The electrode was electrochemically treated by cycling the potential between −0.3 and +1.5 V in the 0.1 mol L^{-1} H_2SO_4. Finally, the electrode was rinsed with distilled water and dried in a nitrogen stream and was ready for use.

At first, 10 μl of 2 mmol L^{-1} cysteamine solution was spread on the gold electrode surface for 2 h to form a cysteamine monolayer. After rinsing with distilled water, the functionalized surface was soaked in 2.5% glutaraldehyde (GA) solution for 3 h, and then was coated with 10 μl of CHITs hydrochloric acid solution (0.5 wt%, pH = 5) for 2 h. Subsequently, the CHITs-modified electrode was submerged into the AuNPs solution overnight to allow the AuNPs to chemisorb onto the surface, and washed with distilled water to thoroughly remove the adhesive AuNPs. Then 10 μl of the growth solution containing 1.8×10^{-4} mol L^{-1} $HAuCl_4$, 7.4×10^{-2} mol L^{-1} CTAB, and 4×10^{-4} mol L^{-1} NADH was dropped on the Au seeds-CHITs-modified electrode for 1 h to initiate the seed-mediated growth process. The procedure of the fabrication of sensing

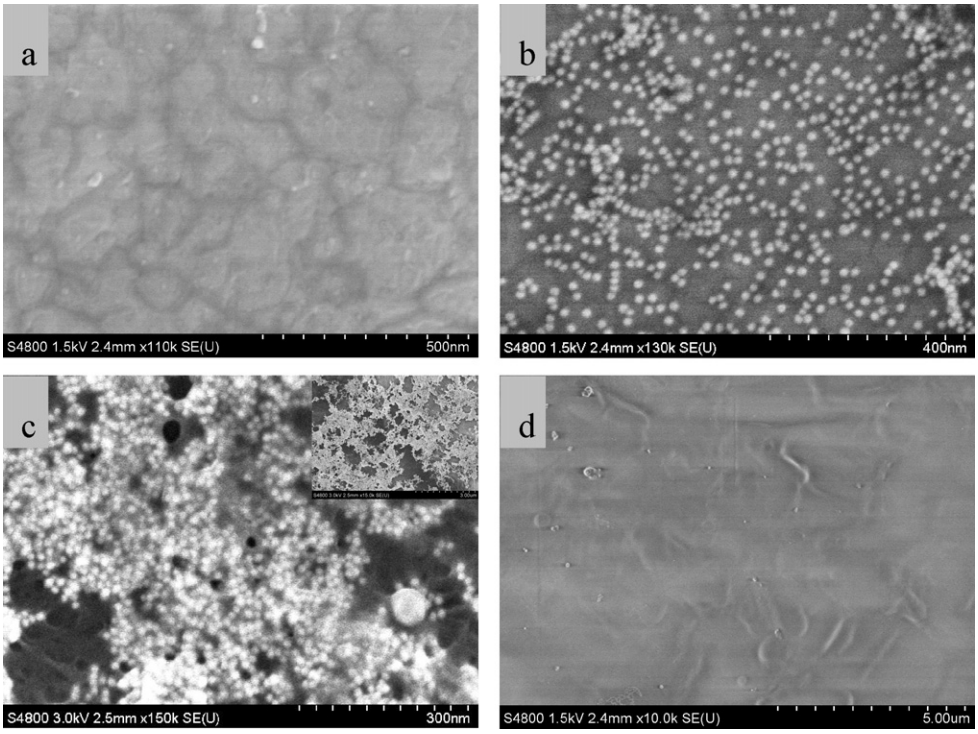

Fig. 2. SEM images of sensing interface: (a) Cys-GA-CHITs modified electrode; (b) Au seeds-modified electrode; (c) coral-shaped AuNPs (C-AuNPs) at a high magnification, insert shows the coral-shaped AuNPs at a low magnification; (d) without adding the Au seeds.

interface was performed at 37 °C throughout the experiment. The modified electrode was denoted as Au/Cys-GA-CHITs/Au seeds/C-AuNPs; other denotations are made in a similar manner.

2.4. Electrochemical measurements and hIgG detection

Goat anti-hIgG (10 μl) was pipetted onto the modified electrode for 1 h, after rinsing with distilled water, 10 μl of 2% BSA solution was added for 1 h to cover the nonspecific sites. Subsequently, the electrode was covered with 10 μl of hIgG for 1 h followed by dropping 10 μl of goat anti-hIgG-HRP for 40 min. Amperometric measurements of immunoassay was performed in 5 ml of PBS (10 mmol L^{-1}, 0.1 mol L^{-1} KCl, pH 7.4) by applying a working potential of −0.4 V under constant stirring. When transient currents became stable, 10 μl of 1 mol L^{-1} H_2O_2 was quickly added.

3. Results and discussion

3.1. Amperometric response of H_2O_2 biosensor

Amperometric response was observed in the absence (curve a) and presence (curve b) of 1 μmol L^{-1} hIgG. As shown in Fig. 1, in the absence of hIgG, relatively low amperometric response was observed while the response increased enormously after addition

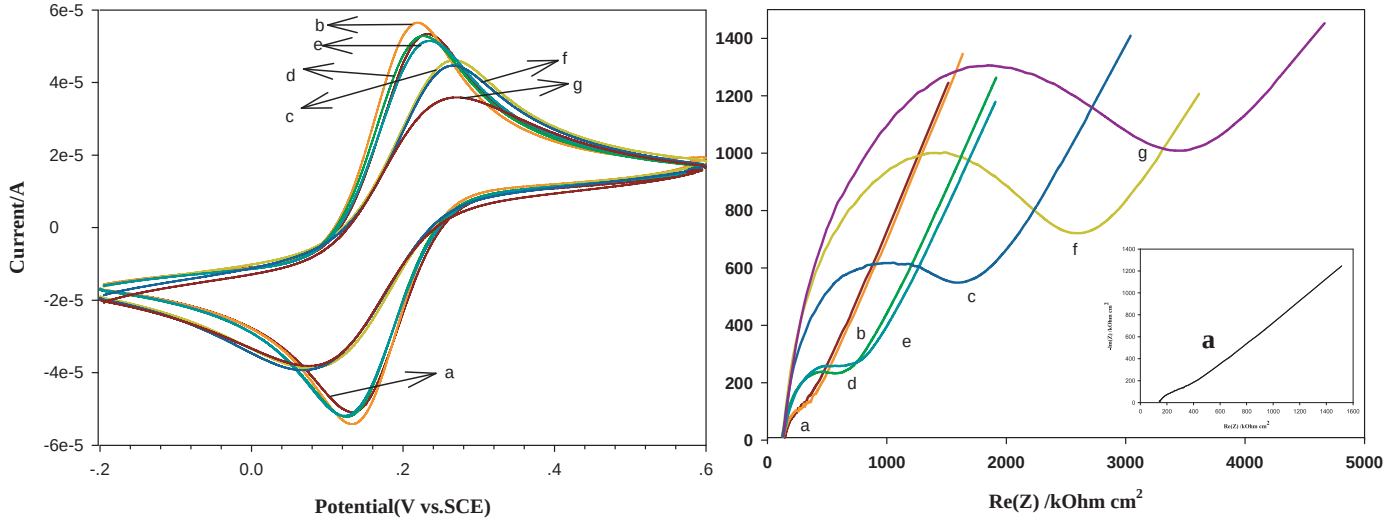

Fig. 3. Nyquist diagrams of (A) cyclic voltammograms and (B) electrochemical impedance for the different modification stages: (a) bare Au electrode; (b) Cys modified electrode; (c) Cys-GA modified electrode; (d) Cys-GA-CHIT modified electrode; (e) C-AuNPs modified electrode; (f) antibody-immobilized electrode; (g) antigen recognized electrode. All measurements were performed in 0.1 mol L^{-1} PBS (pH 7.4) and 5 mmol L^{-1} $[Fe(CN)_6]^{3-}$/$[Fe(CN)_6]^{4-}$.

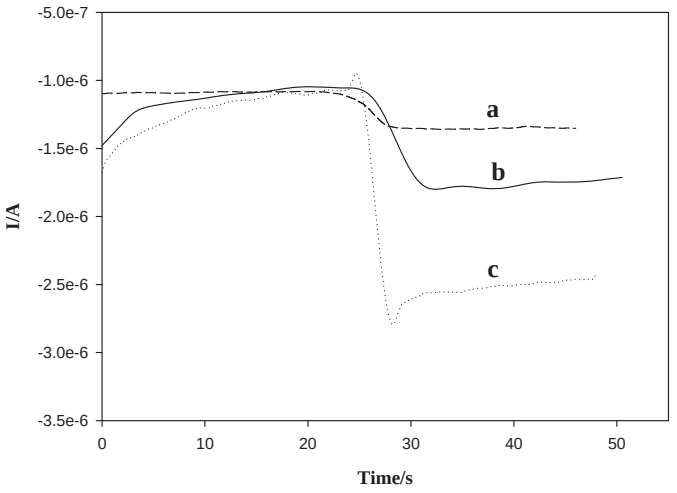

Fig. 4. Amperometric responses of H_2O_2: (a) in the absence of Au seeds, (b) in the absence of the growth solution, and (c) in the presence of Au seeds and growth solution.

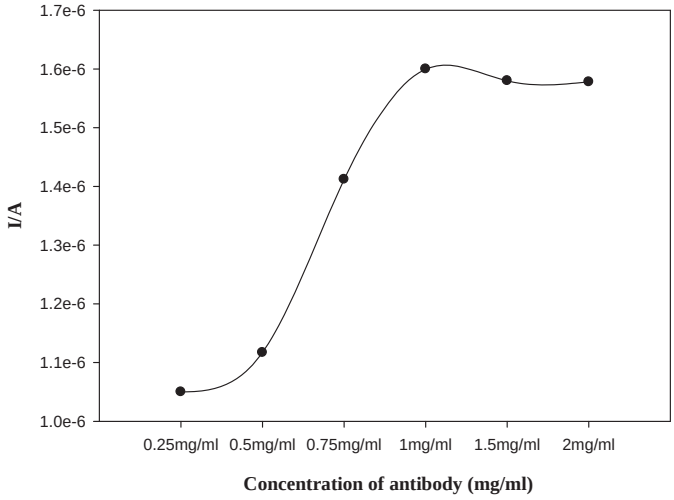

Fig. 6. Effect of IgG antibody concentration on amperometric curve response of H_2O_2. Antigen concentration: 1 μg/ml and growth time: 60 min.

of hIgG. This result might be interpreted as that in the presence of the hIgG, HRP enzyme brought about by the specific immune response could efficiently catalyze thousands of reduction reactions of hydrogen peroxide (H_2O_2), leading to significantly amplified electrochemical current signal [18]. It is well known that H_2O_2 is electrocatalytically transformed on HRP-modified electrodes [19,20]. In the absence of the hIgG, only a small quantity of HRP labelled antibodies adsorb on the AuNPs resulting low amperometric response. It may be considered as the background current intensity originating from nonspecific binding of HRP labelled antibodies to the surface.

3.2. Characterization of morphology at Au electrode

Although the Scheme 1 can well explain the above mentioned results, the model still needs further experimental verification. Therefore, the morphology of Cys-GA-CHITs/Au seeds/C-AuNPs electrode at different stages was investigated by using scanning electron microscopy (SEM). As shown in Fig. 2b, Au seeds linked to the resulting electrode, the particles on the nanometer scale scattered evenly on the Cys-GA-CHIT modified electrode surface were observed. After dropping the growth solution (NADH, CATB

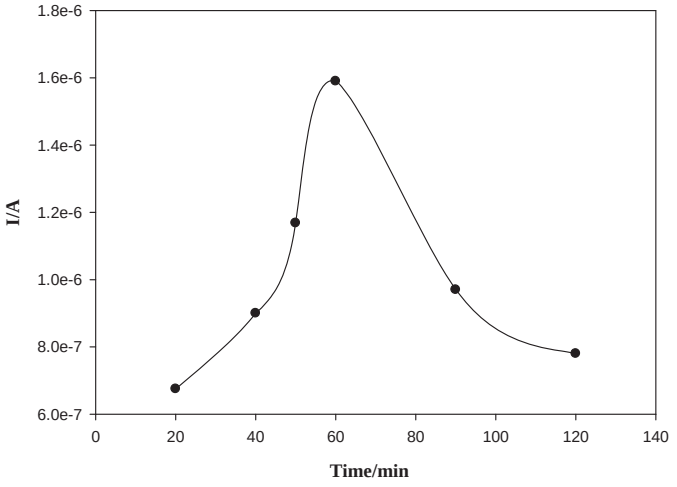

Fig. 5. Effect of growth time on amperometric curve response of H_2O_2. Antibody concentrations: 1 mg/ml, and antigen concentration: 1 μg/ml.

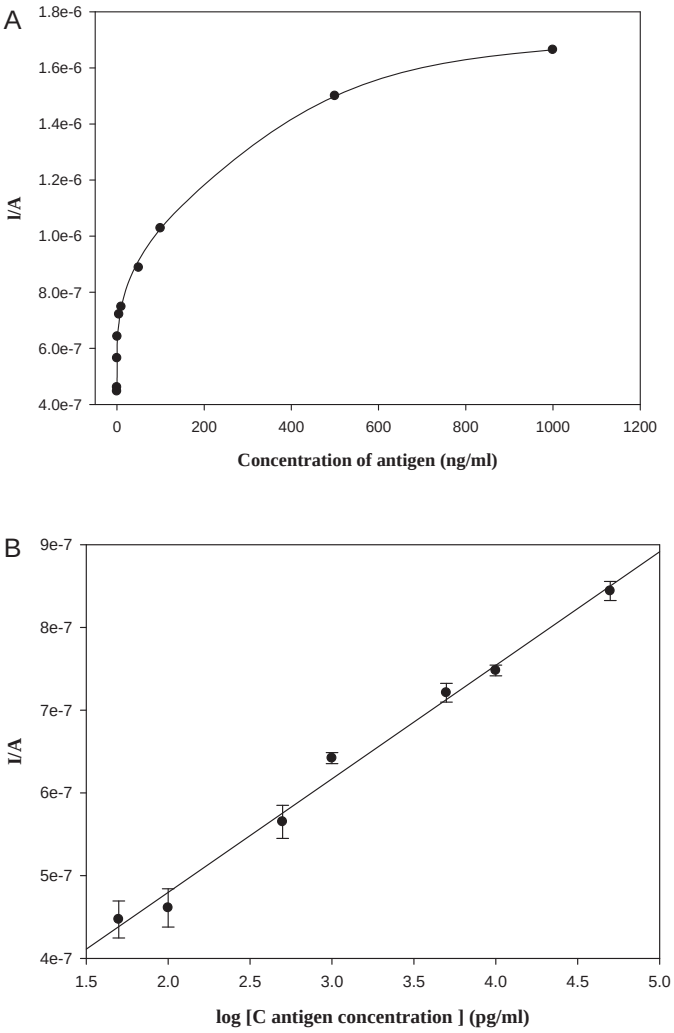

Fig. 7. The linear relationship between the change of current response (A) and log of IgG concentration (B) under optimized conditions (concentration of goat anti-hIgG: 1 mg/ml, growth time: 60 min). The error bars indicated the standard deviations of three independent experiments.

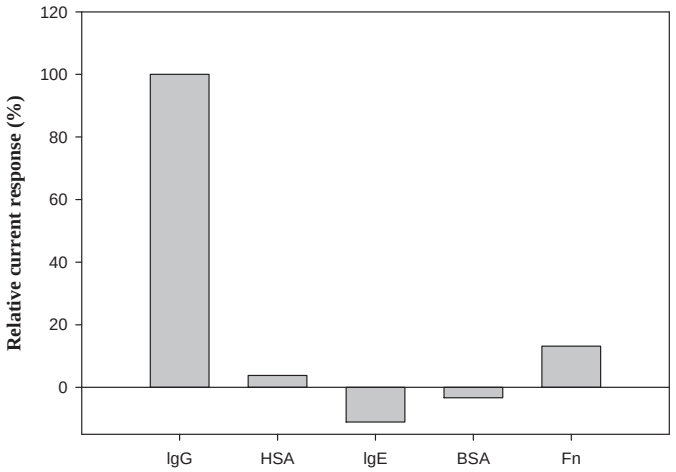

Fig. 8. The baseline-subtracted amperometric *i–t* curve response of the proposed sensing system after being exposed to five different proteins dissolved in PBS (10 m mol L^{-1}, 0.1 M KCl, pH 7.4): (1) 0.5 μg/ml IgG; (2) 5 μg/ml HSA; (3) 14 μg/ml IgE; (4) 10 mg/ml BSA; (5) 5 μg/ml Fn.

and Au^{3+}) to the resulting electrode, the AuNPs tended to cluster together, forming a coral-like large 3D clusters (seen in Fig. 2c), with a large surface area. However, without adding the Au seeds, no particles but a uniform and smooth monolayer were observed (Fig. 2d).

3.3. Electrochemical characterization of the modified gold electrode

The modified electrodes were analyzed using cyclic voltammetric and alternating current impedance measurements. Cyclic voltammograms (CV) behavior was obtained in 5 ml of PBS (10 mmol L^{-1}, pH 7.4) containing 5 mmol L^{-1} $K_4[Fe(CN)_6]$, 5 mmol L^{-1} $K_3[Fe(CN)_6]$ and 0.1 mol L^{-1} KCl, in the range from −0.2 to +0.6 V at a scan rate of 100 mV s^{-1}. The alternating current impedance was carried out in the same solution with a frequency range from 1 to 100,000. Fig. 3A shows the cyclic voltammograms (CV) of the modified gold electrode. There was a couple of redox on the bare gold surface during cycling of potential (a) and increased slightly after Cys assembled on the gold electrode (b). Because GA obturated many amino groups of Cys, a decrease of current intensity was observed (c). However, an intensive positively charged CHITs monolayer which was formed by using GA as a cross-linking reagent led to peak current increased, for the CHITs-modified gold electrode surface contains large quantity of amino groups (d). Introducing the Au seeds and growth solution (e) did not change the conductivity very much, as the conductivity of the modified electrode was already quite nice. Afterward, goat anti-hIgG was covalently linked to the modified gold electrode. Due to good biocompatibility of CHITs and C-AuNPs, the specific immune response take place between hIgG and goat anti-hIgG on Au/Cys-GA-CHITs/Au seeds/C-AuNPs electrode surface. The immune complexes block the diffusion of ferricyanide toward the conductive electrode surface, which reduced the peak current (f). Fig. 3B shows the impedance of stepwise assembly, the results obtained were identical with those from cyclic voltammograms.

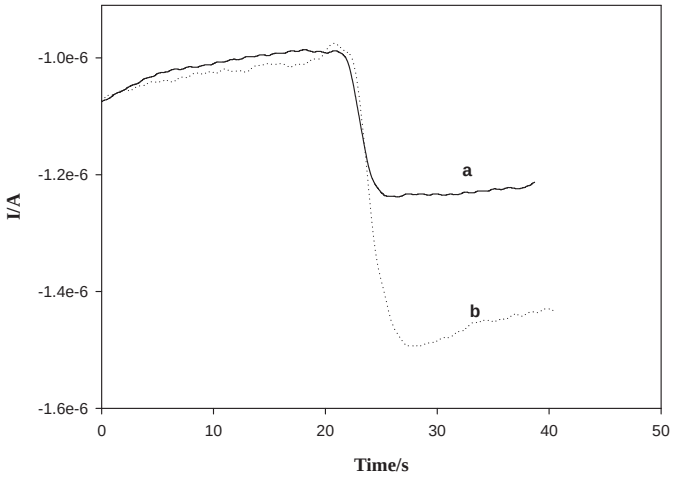

Fig. 9. Amperometric responses of H_2O_2: in the absence (a) and presence (b) of 10 μg/ml hIgG in human serum (100-fold diluted).

3.4. Amplification of electrochemical signal

CHITs were explored for the amplification of amperometric response making use of its abundant amino groups [21]. Due to the strong electrostatic interactions of gold nanoparticles for amino functional group, the Au seeds were adsorbed on the modified electrode. When Au NP interface is soaked in the growth solution, the surface density of the Au NP become higher, the catalytic deposition of gold on the NPs is enhanced [22]. The large surface area made it possible to adsorb a large number of antibody molecules. Therefore, significantly amplified electrochemical signal was detected. As shown in Fig. 4, in the absence of the growth solution (NADH, CATB, Au^{3+}), small amperometric response was found (curve b), and when no Au seeds was existed, smaller amperometric response was observed (curve a). However, in the presence of both Au seeds and growth solution, amperometric response became rather high due to the large surface area (curve c), indicating that the coral-shaped gold nanoparticles (C-AuNPs) synthesized by using a seed-mediated growth method are indeed able to amplify the signal. The results were in complete agreement with those from the SEM.

3.5. Effect of the growth time

The properties of metal nanoparticles are generally dependent on several structural parameters, including composition, crystallinity, nanoparticle size, and interparticle distance [23]. The number of gold particles on the electrode surface was an important parameter for significantly improving the performance of the H_2O_2 biosensor [24]. Herein, the dependence of the growth time on amperometric response was studied. Fig. 5 shows the effect of the growth time over the range from 20 min to 120 min in the antibody concentration of 1 mg/ml, and antigen concentration of 1 μg/ml. Owing to the increased surface area of protuberant spherical porous nanostructure, as shown in Fig. 5, a peak current increased gradually with augment of the growth time. Coral-shaped gold nanoparticles on the surface could improve the sensitivity of hIgG detection, because more goat anti-hIgG antibody molecules can be adsorbed onto the C-AuNPs modified electrode surface. However, the peak current tended to a maximum value at 60 min and sharply decreased after that time because excessive deposition of Au onto the Au agglomerates may result in porous nanostructure failure [10]. Therefore, 60 min was chosen for the growth time.

3.6. Effect of goat anti-hIgG antibody concentration

The effect of the concentration of goat anti-hIgG was also investigated to obtain the high assay sensitivity. The concentration of goat anti-hIgG ranges from 0.25 mg/ml to 2 mg/ml in the antigen concentration of 1 μg/ml, and growth time of 60 min. As depicted in Fig. 6, the peak current intensity increased briskly with the

concentration of goat anti-hIgG since more goat anti-hIgG can strong adsorbed on the C-AuNPs surface due to the large specific surface area. When the concentration of goat anti-hIgG reaches to 1 mg/ml, a plateau was observed. Therefore, 1 mg/ml goat anti-hIgG was used for the incubation.

3.7. Analytical characteristics performance of sensing system

To test whether proposed biosensor could be used for hIgG quantitation, a series of different antigen concentration were used under the optimized conditions. As shown in Fig. 7, the peak current intensity increased with increasing hIgG concentration. The change of peak current intensity exhibited a linear correlation to the logarithm of the concentration of hIgG. The linear equation is $\Delta I_{peak} = 2.053 \times 10^{-7} \log C + 1.372 \times 10^{-7}$ with the correlation coefficient of 0.990. The linear calibration range of hIgG is from 50 pg/ml to 50 ng/ml and the detection limit is 5 pg/ml obtained by 3 S/N. Such a good performance can be attributed to the nano–bio combination film with abundant adsorbing sites and large surface area which can increase loading quantity assembling of protein molecules and transfer electron very well, thereby, can significantly improve the performance of biosensing. Besides, the enzyme amplification reaction also promotes the sensitivity and extends the detection range. Therefore, improved sensitivity is comparable or better than that of some previous correlative work [25–28].

3.8. Specificity

In our experiments, BSA (bovine serum albumin), HSA (human serum albumin), fibronectin (Fn) and human IgE (hIgE) were chosen to investigate the specificity of the H_2O_2 biosensor. As depicted in Fig. 8, the peak current intensity changed less for other protein, while a significant current change was observed for hIgG. The interaction of other antigens had a negligible effect on the current change. In other words, our design biosensor has good specificity towards other protein. To test the practicality of this sensor, we conducted analyses of hIgG in human serum, a complex media that contained a variety of proteins and other serious interference. The hIgG was added to the diluted (100-fold) serum samples. Upon addition of 10 μg/ml hIgG, as shown in Fig. 9, a relatively high amperometric response was observed, while low amperometric response was detected in the absence of target under the same condition. The result demonstrated that the newly proposed sensor showed good properties in possible practical applications.

4. Conclusion

The amperometric biosensor based on Cys-GA-CHIT/Au seeds/C-AuNPs allows not only high enzyme loading with unique conformation but also easy electron transfer owing to the orderly spatial orientation and large surface area. Coral-shaped AuNPs (C-AuNPs) with large surface area greatly increase assembling loading and can transfer electron very well, thereby significantly improving the performance of the biosensor. Besides, the enzyme amplification reaction also promotes the sensitivity and extends the detection range. The advantages of the developed biosensor, such as small sample size, simplicity, low cost, sensitive detection and fast response make it an attractive alternative platform for the direct immunoassay of hIgG or other biomolecules.

Acknowledgements

This research was supported by the National Natural Science Foundation of China (Grants no. 21035001 and 90817101), and the "973" National Basic Research Program of China (2011 CB 911000).

References

[1] P. Ghosh, G. Han, M. De, C.K. Kim, V.M. Rotello, Adv. Drug Del. Rev. 60 (2008) 1307–1315.
[2] N. Wangoo, K.K. Bhasin, R. Boro, C.R. Suri, Anal. Chim. Acta 610 (2008) 142–148.
[3] M.-C. Daniel, D. Astruc, Chem. Rev. 104 (2004) 293–346.
[4] Y.B. He, H.Q. Luo, N.B. Li, Biosens. Bioelectron. 22 (2007) 2952–2957.
[5] H. Cai, C. Xu, P. He, Y. Fang, J. Electroanal. Chem. 510 (2001) 78–85.
[6] Y. Xiao, H.-X. Ju, H.-Y. Chen, Anal. Chim. Acta 391 (1999) 73–82.
[7] A. Doron, E. Katz, I. Willner, Langmuir 11 (1995) 1313–1317.
[8] C.J. Murphy, T.K. Sau, A.M. Gole, C.J. Orendorff, J. Gao, L. Gou, S.E. Hunyadi, T. Li, J. Phys. Chem. B 109 (2005) 13857–13870.
[9] L. Yuan, M. Yang, F. Qu, G. Shen, R. Yu, Electrochim. Acta 53 (2008) 3559–3565.
[10] J.-L. He, Z.-S. Wu, P. Hu, S.-P. Wang, G.-L. Shen, R.-Q. Yu, Analyst 135 (2010) 570–576.
[11] T.K. Sau, C.J. Murphy, J. Am. Chem. Soc. 126 (2004) 8648–8649.
[12] R.A.A. Muzzarelli, Chitin, Pergamon Press, Oxford, 1977.
[13] W.F. Stevens, M.S. Rao, S. Chandrkrachang, Chitin and Chitosan, Asian Institute of Technology, Bangkok, Thailand, 1996.
[14] R.H. Chen, H.C. Chen, Advances in Chitin Science, National Taiwan Ocean University, Keelung, Taiwan, 1998.
[15] W.L. Meyer, Y. Liu, X.-W. Shi, X. Yang, W.E. Bentley, G.F. Payne, Biomacromolecules 10 (2009) 858–864.
[16] Q. Sheng, K. Luo, J. Zheng, H. Zhang, Biosens. Bioelectron. 24 (2008) 429–434.
[17] M.-F. Huang, Y.-C. Kuo, C.-C. Huang, H.-T. Chang, Anal. Chem. 76 (2004) 192–196.
[18] G. Liu, Y. Wan, V. Gau, J. Zhang, L. Wang, S. Song, C. Fan, J. Am. Chem. Soc. 130 (2008) 6820–6825.
[19] Z. Wu, L. Chen, G. Shen, R. Yu, Sens. Actuators B: Chem. 119 (2006) 295–301.
[20] B. Limoges, J.M. Saveant, D. Yazidi, J. Am. Chem. Soc. 125 (2003) 9192–9203.
[21] S.-B. Zhang, Z.-S. Wu, M.-M. Guo, G.-L. Shen, R.-Q. Yu, Talanta 71 (2007) 1530–1535.
[22] V. Pavlov, Y. Xiao, B. Shlyahovsky, I. Willner, J. Am. Chem. Soc. 126 (2004) 11768–11769.
[23] C.A. Mirkin, R.L. Letsinger, R.C. Mucic, J.J. Storhoff, Nature 382 (1996) 607–609.
[24] S. Sankaran, S. Panigrahi, S. Mallik, Sens. Actuators B 137 (2009) 736–740.
[25] Y. Zhou, Y. Zhang, C. Lau, J. Lu, Anal. Chem. 78 (2006) 5920–5924.
[26] G. Liu, J. Wang, H. Wu, Y. Lin, Anal. Chem. 78 (2006) 7417–7423.
[27] A. Ambrosi, M.T. Castañeda, A.J. Killard, M.R. Smyth, S. Alegret, I. Arben Merkocü, Anal. Chem. 79 (2007) 5232–5240.
[28] S. Wang, Z. Wu, F. Qu, S. Zhang, G. Shen, R. Yu, Biosens. Bioelectron. 24 (2008) 1020–1026.